INSTITUTE OF PHYSICS PUBLISHING JOURNAL OF PHYSICS: CONDENSED MATTER

J. Phys.: Condens. Matter **15** (2003) 8465–8484 PII: S0953-8984(03)66139-4

Excited states in the infinite quantum lens potential: conformal mapping and moment quantization methods

Arezky H Rodríguez[1], **Carlos R Handy**[2] **and C Trallero-Giner**[1]

[1] Department of Theoretical Physics, University of Havana, 10400, Havana, Cuba
[2] Department of Physics and Center for Theoretical Studies of Physical Systems, Clark Atlanta University, Atlanta, GA 30314, USA

Received 12 July 2003
Published 25 November 2003
Online at stacks.iop.org/JPhysCM/15/8465

Abstract

The conformal mapping method (CMM) and the eigenvalue moment method (EMM) are employed to study the eigenvalue problem defined by a free particle in a quantum lens geometry. The characteristics of the spectrum and the corresponding spatial properties of wavefunctions are studied for varying symmetry quantization numbers and lens parameter values. It is shown that the states belong to two independent Hilbert subspaces corresponding to even and odd azimuthal, m, quantum numbers. The CMM analysis is used to reduce the Dirichlet problem for the Helmholtz's equation into a 2D problem defined by a region with semicircular geometry. This approach allows one to obtain explicit analytical solutions in terms of the lens geometry. In the case of small geometry deformations (relative to the semicircular case), the solutions can be found by a perturbative method. The exact and approximate solutions are compared for different values of the lens parameters. We compare these results with those derived through the EMM approach, which, although more computationally expensive, can yield converging lower and upper bounds. The particular formulation developed here differs significantly from an earlier application of EMM to the ground state case (within each symmetry class). Accordingly, we develop the new formulation and apply it to a limited number of states in order to confirm the results derived by the other, aforementioned, methods.

1. Introduction

The interest in quantum dots (QDs) has recently increased due to the novel properties these zero-dimensional structures exhibit, as a consequences of their particular spatial confinement properties (see [1] and references therein). These novel structures are obtained by interrupted growth in strained semiconductors. Different techniques have been used to study their shape

and size, suggesting that under certain growing conditions, the self-assembled QDs are lens shaped [2–10] with a spherical cap of height b, and circular cross section of radius a (see [11]).

In the case of InAs islands grown on a GaAs surface, the in-plane diameters are typically less than 30 nm, while their heights are below 10 nm, showing a small height-to-area aspect ratio. Differential capacitance [12, 13], magnetic-conductance [14], and optical experiments [2, 15] demonstrate that the electronic states are strongly confined inside such structures. Different possible applications [16] make it important to understand the dependence of the ratio b/a on the electronic structure of the QDs. Nevertheless, the lens geometry itself represents a serious mathematical problem, since readily obtainable solutions for the eigenstates and eigenvalues are not known.

Two solution methods are proposed here. The first involves conformal transformation (CT) analysis, whereas the second is made possible by the eigenvalue moment method (EMM). The CT method is described in [17], and involves mapping the quantum lens (QL) domain into a semi-spherical QD. This type of approach has been used on other types of geometries [18–22]. Within the transformed domain one is able to determine a basis of functions for the corresponding Hilbert space. Using this, in [17] a modified Rayleigh–Schrödinger perturbation theory was developed in order to evaluate the energy levels up to second order, and the wavefunctions up to first order in the $(1 - b/a)$ parameter. This approach is useful for a small range of values of b/a close to 1. Hence, the eigenvalue problem valid in a large range of b/a values is still an open question. Here, the previous results are extended, taking into account a matrix diagonalization procedure valid for b/a values ranging between (0, 1].

Besides the use of conformal analysis, it also possible to use an affine map invariant, variational analysis, in order to generate converging lower and upper bounds for the excited states. This is the essence of the EMM formalism introduced in [11]. An affine map transformation involves rescaling, translating, and rotating a given region of space. Any variational procedure, invariant to affine transforms of the sampling function space, will be very efficient in analysing singular problems sensitive to multiscale contributions. Within the EMM procedure, the sample function space is made up of polynomials (which are trivially invariant under affine transformations). Accordingly, implementation of EMM is done within a power moment's representation.

We emphasize an important requirement of the EMM approach. One must work within a configuration representation in which the physical solution is uniquely nonnegative and bounded (although here, the latter is easily achieved because the lens domain is compact, and the physical solutions have unique boundary conditions). In the earlier work in [11], we focused on the ground state, within each symmetry class, for which the physical solutions always satisfy the required conditions.

In the present case of excited states, since the physical solutions have varying signature, Φ, we must determine a crude *lower bound* to the wavefunction, $-c < \min\{\Phi\}$, resulting in the positive configuration $\Phi(\vec{r}) + c$. If we know such a (rough) lower bound to the wavefunction, then the EMM theorems guarantee that one can generate *converging* lower and upper bounds to the individual, excited, states.

We do not know of any convenient method by which to determine, exactly, such approximate lower bounds to the wavefunction. Instead, we determine such wavefunction lower bounds, *empirically*, by implementing the EMM procedure and testing for consistency with the EMM constraints, to sufficiently high expansion order (within our computing power resources). Thus, we are communicating an exact theory, which, if the empirically determined wavefunction lower bound is correctly determined (i.e. that it is indeed a lower bound), will result in true bounds for the excited state energy. However, it may happen that the 'c' value empirically determined is not exactly (but is close to) a true wavefunction lower bound. In this

case, the spectral bounds generated are not true bounds, but give a sense of the reliability of this method, as a spectral estimation procedure.

In all cases, we compare both methods communicated here with each other. Thus, in addition to solving an important physical problem, the analysis presented here underscores the theoretical importance of determining (crude) lower bounds to the wavefunction, since these can lead to high precision (tight) lower and upper bounds to the discrete state energies.

The paper is organized as follows. In section 2 we discuss the conformal mapping method (CMM). The energy levels and associated wavefunctions are given as a function of the parameter lens deformation b/a. Section 3 is devoted to the moment quantization, EMM approach. It includes a comparison between both studied mathematical treatments of the QD lens geometry. Our conclusions appear in section 4. Much of the detail of the EMM approach, particular to the present case of excited states, appears in the appendix.

2. Conformal mapping method

Assuming a one particle Hamiltonian model with effective mass m, the eigenvalue problem fulfilling the Dirichlet boundary condition in a lens geometry is described by the stationary Schrödinger equation

$$\nabla^2\Phi + \lambda\Phi = 0, \tag{1}$$

where $\lambda = (2m/\hbar^2)E$ and E is the eigenenergy. The axial symmetry of the QD allows one to write the eigenvalue problem of equation (1) in polar coordinates

$$\nabla^2 f(r_1,\theta_1) + \left(\lambda - \frac{m^2 - 1/4}{r_1^2\sin^2\theta_1}\right) f(r_1,\theta_1) = 0, \tag{2}$$

with

$$\Phi = \frac{f(r_1,\theta_1)}{\sqrt{r_1\sin\theta_1}}\frac{\mathrm{e}^{\mathrm{i}m\phi}}{\sqrt{2\pi}}, \tag{3}$$

where $0 \leqslant \theta_1 \leqslant \pi/2$ and $0 \leqslant \phi < 2\pi$. The lens domain presents a mirror symmetry with respect to the z-axis. In consequence the space of solutions can be classified according to the values of the quantum number m, and the eigensolutions of equation (2) are taken as *even* or *odd* functions.

The domain of solutions to the QL geometry does not allow one to find explicit forms for the eigenstates of equation (2). To obtain explicit analytic solutions, the CMM is proposed, keeping the corresponding lens symmetry with respect to the z-axis, and preserving the parity of the wavefunction $f(\boldsymbol{r}_1)$. In [17] a CT which maps the 2D QL domain into a semicircular one is described. Thus, the eigenvalue problem (2) is mapped into the problem

$$\nabla^2 f^{(\beta)}(r,\theta) + \mathcal{J}_\beta(r,\theta)\left(\lambda(\beta) - \frac{m^2 - 1/4}{\mathcal{X}_\beta^2(r,\theta)}\right) f^{(\beta)}(r,\theta) = 0, \tag{4}$$

$$f^{(\beta)}(a,\theta) = f^{(\beta)}(r,\pm\pi/2) = 0, \tag{5}$$

where $\beta = b/a$ and $\mathbf{r} = (r,\theta)$ are the new coordinates within the semicircle of radius a. The Jacobian of the transformation, $\mathcal{J}_\beta$, and $\mathcal{X}_\beta$ are mathematical objects which contain the information of the lens geometry [17]. It should also be noted that for $\beta \to 1$, the Jacobian becomes $\mathcal{J}_\beta \to 1$, while $\mathcal{X}_\beta$ equals $r\sin\theta$. In addition, equation (4) reduces to (2) for a QD with semi-spherical shape. It is also important to state that due to the reduction of the symmetry in the lens domain, the degeneracy with respect to the azimuthal quantum number, m, in the semicircular case, is broken; but the states with $\pm m$ projection remain with the same eigenenergy (two-fold degeneracy).

To find the solution of equation (4) in the new semicircular domain, the function $f^{(\beta)}(r,\theta)$ will be expanded in terms of a complete set of orthonormal eigenfunctions $\{f^{(0)}_{n,l,m}\}$, fulfilling the 2D Dirichlet boundary conditions on a semicircle (see [17]).

$$f^{(\beta)}_{N,m}(r,\theta) = \sum_{i=\{n,l\}}^{\infty} C^{(\beta)}_i(N,m)\, f^{(0)}_{i,m}(r,\theta). \tag{6}$$

Here, $f^{(0)}_{i,m}(r,\theta) = f^{(0)}_{n,l,m}(r,\theta) = \sqrt{\sin\theta}\, J_{l+1/2}(\mu_{n,l}\, r/a)\, P_l^{|m|}(\cos\theta)$, where $\mu_{n,l}$ is the nth zero of Bessel function $J_{l+1/2}(\mu^{(l)}_n) = 0$, and $l = 0, 1, \ldots; -l \leqslant m \leqslant l$. The states are labelled by N, m, where N labels the new electronic states in increasing order of the energy $E_{N,m}$ at $b/a = 1$.

To fulfill the boundary conditions at $\theta = \pm\pi/2$, we require $|l - m| = odd$ number, restricting the space of solutions of equation (4) with respect to the spherical domain. Notice that for a given β the solutions of equation (4) have to be solved for each value of the quantum number m. That is, different levels, with differing values of m, do not 'see' each other, and the sum in equation (6) is only over quantum numbers $\{n, l\}$. Thus, the set of eigenenergies for a given m cannot cross each other; and anticrossing effects can be expected as a function of the parameter β. Nevertheless, eigenenergies with different values of m can cross, for particular values of β.

Taking the former relation in equation (4), multiplying by $|f^{(0)}_{j,m}\rangle = |j\rangle$ and integrating over the entire domain, one obtains

$$\sum_{i=\{n,l\}}^{\infty} C^{(\beta)}_i(N,m)\left\{(\mu_i)^2\delta_{i,j} + \left(m^2 - \frac{1}{4}\right)\langle j|\frac{\mathcal{J}_\beta}{\mathcal{X}^2_\beta} - \frac{1}{r^2\sin^2\theta}|i\rangle - \lambda(\beta)\langle j|\mathcal{J}_\beta|i\rangle\right\} = 0. \tag{7}$$

Equation (7) is an infinite generalized eigenvalue problem for the eigenvalue $\lambda(\beta)$ and eigenfunction $\{C_i(\beta)\}$. Its solutions were first obtained in [17] using a modified Rayleigh–Schödinger perturbation formalism when the lens domain is different from a semicircle. Solutions were reported for the eigenvalues up to second order in the perturbation parameter $(1 - \beta)$. This approach is strictly valid for small deformation of the semi-spherical dot into a lens configuration. To complete the study of the spectrum of the Schödinger equation in a lens geometry, it is necessary to find better ways to calculate the eigenvalues and eigenfunctions for a wide range of b/a values. Here, we will find the eigensolutions $f^{(\beta)}_{N,m}$ in terms of the truncated basis set, $\{f^{(0)}_{i,m}\}$ $(i = 1, \ldots, I)$, defining the finite-dimensional, Hill determinant, eigenenergy equation [23]

$$\|\mathcal{M}^{(I)}(\lambda(\beta))\| = 0, \tag{8}$$

where $\mathcal{M}^{(I)}_{i,j}$, $(i, j = 1, 2, \ldots, I)$ are the matrix elements given in equation (7). Since the functions $\{f^{(0)}_{i,m}\}$ define a complete set for the Schrödinger equation, defined on a semi-spherical domain obeying the Dirichlet boundary conditions, the roots of the determinant (8) converge to the exact eigenenergies of equation (1) and $\lim_{I\to\infty} \lambda^{(I)}_{N,m}(\beta) = \lambda_{N,m}(\beta)$ [23].

To solve equation (8) numerically, the first 100 values for μ_i were sorted in increasing order ($i = 1$ corresponds to $n = 1, l = 1$, $i = 2$ to $n = 1, l = 2$, etc) and the matrix elements of equation (7) were calculated for β ranges between 0.1 and 0.98 using an adaptable Gauss–Kronrod integration method with absolute and relative error ϵ smaller than 10^{-6}. The defined map $(n, l) \to i = i(n, l)$ and the rearranged eigenfunctions $f^{(0)}_{i,m}$ allow one to optimize the numerical contribution of the matrix element $\mathcal{M}^{(I)}_{i,j}$ to a given eigenvalue $\lambda(\beta)$. Thus, a radius of convergence $\delta(\beta)$ for a particular $\lambda(\beta)$ value can be defined according to the desired accuracy. As b/a decreases, the radius of convergence increases, as one would expect. In our case, a 100×100 matrix is enough to calculate the first 30 eigenvalues for b/a ranging

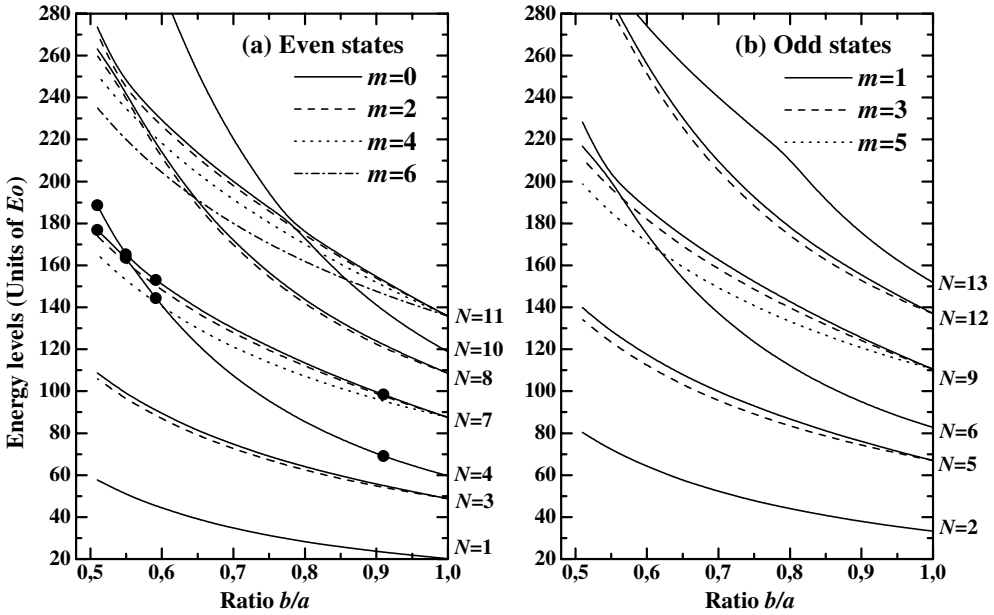

Figure 1. The first 24 energy levels as a function of the lens deformation parameter b/a calculated solving the Hill determinant (8). (a) Even states. (b) Odd states. The energy levels are labelled by the quantum number N, m, where N labels the new electronic states in increasing order of the energy at $b/a = 1$.

between 0.5 and 0.98 with a relative precision $\epsilon = 10^{-3}$. For values of b/a smaller than 0.5 the range of the matrix has to be increased to obtain the same accuracy; that is, in the range of $0.1 < b/a < 0.5$ and for a 100×100 matrix only the first five eigenvalues have the relative precision $\epsilon = 10^{-3}$. In the previous case we need to increase the order of the matrix to obtain a better accuracy.

Figure 1 shows the dependence of the first 24 energy levels in units of $E_0 = \hbar/2ma^2$ on the ratio b/a. The energy levels are labelled according to their behaviour at $b/a = 1$ (semi-spherical case) with the pair numbers (N, m). In figure 1(a) the even states corresponding to the quantum numbers $m = 0, 2, 4$, and 6 are represented, while in figure 1(b) the odd states with $m = 1, 3$, and 5 are shown. The lower levels exhibit a weaker dependence on the decreasing b/a ratio, while the upper levels strongly deviate from the semi-spherical case, as expected. The breaking of the degeneracy for energy levels $N = 3, 5, 7, 8, 9, 11$ and 12 at $b/a \neq 1$ is manifested clearly. For a given quantum number N, the large m values have the lower energies. One can also see the energy level interactions for those states with the same value of the quantum number m (i.e. between levels $N = 4, m = 0$ and $N = 7, m = 0$ at $b/a \approx 0.56$). This anticrossing effect is always present for eigenvalues with the same symmetry (the same quantum number m). Nevertheless, energy states with different m can cross each other when b/a varies. Due to the combined effect of crossing and anticrossing between eigenvalues, a drastic change of energy distribution as a function of the lens deformation is produced. Such complex distributions of levels suggests a complicated behaviour for some of the physical parameters of the system [24].

A comparison between the results obtained by solving the Hill determinant (8) with those reported in [17] using second-order perturbation theory is shown in figure 2. The first five energy levels corresponding to even states with $m = 0$ are plotted in figure 2(a) while the

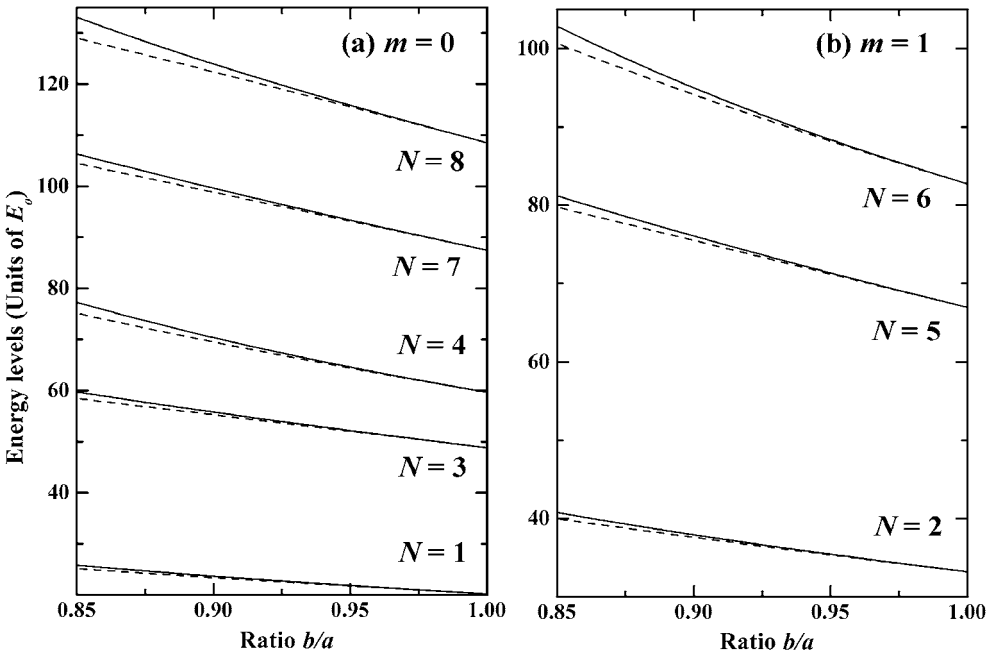

Figure 2. A comparison between the first energy levels as a function of the ratio b/a calculated solving the Hill determinant (8) (straight lines) and using the perturbation method (dashed lines). (a) Energy levels with $m = 0$, $N = 1, 3, 4, 7$ and 8. (b) Energy levels with $m = 1$, $N = 2, 5$ and 6.

first three energy levels for odd states and $m = 1$ are shown in figure 2(b). Good agreement between both methods can be seen for the lower energy levels and values of b/a close to 1. It is also discernible that second-order perturbation theory breaks down for a lens deformation smaller than 0.8 (ground state), while its range of validity is drastically reduced in the case of the excited states. For large deformation of the QL, the perturbation theory must include higher-order terms to provide a better approximation to the exact results.

In figure 3 we show the contour plots of the probability density function (PDF) for eight energy levels and three different values of the b/a ratio. In all cases it can be seen that when b/a decreases the maximum values of the PDF shift to the plane of the lens given by $\theta = \pm\pi/2$. The figure also shows the change of the nodal distribution observed in the higher excited states as the QL deformation is increased (see, for example, states $N = 4, m = 0$ and $N = 6, m = 1$). For these states, the flatter lens geometry provokes a stronger effect on the PDF as a function of the decreasing b/a. This behaviour is explained by their energy dependence on the b/a parameter, where a strong repulsion is observed in figure 1 at $b/a \approx 0.56$. The lens deformation induces coupling between the states $f^{(0)}_{i,m}$ of the semi-spherical geometry.

It is also interesting to explore the behaviour of the probability density for b/a ratio values close to the anticrossing regime for two energy levels. Specifically, the region marked by full dots in figure 1(a), in which two electronic states of even parity anticross, is shown in figure 4. In this region there is also a state with $m \neq 0$ for which their dispersion is unaffected by the presence of the neighboring states (see figure 1(a)), illustrating the independence of states with the quantum number m. The anticrossing effect is clearly seen in figure 4, where a three-dimensional plot of the PDF for the levels $N = 4, m = 0$ and $N = 7, m = 0$ is shown for the chosen values of the b/a ratio. At $b/a = 1$ (not shown), the density of the probability

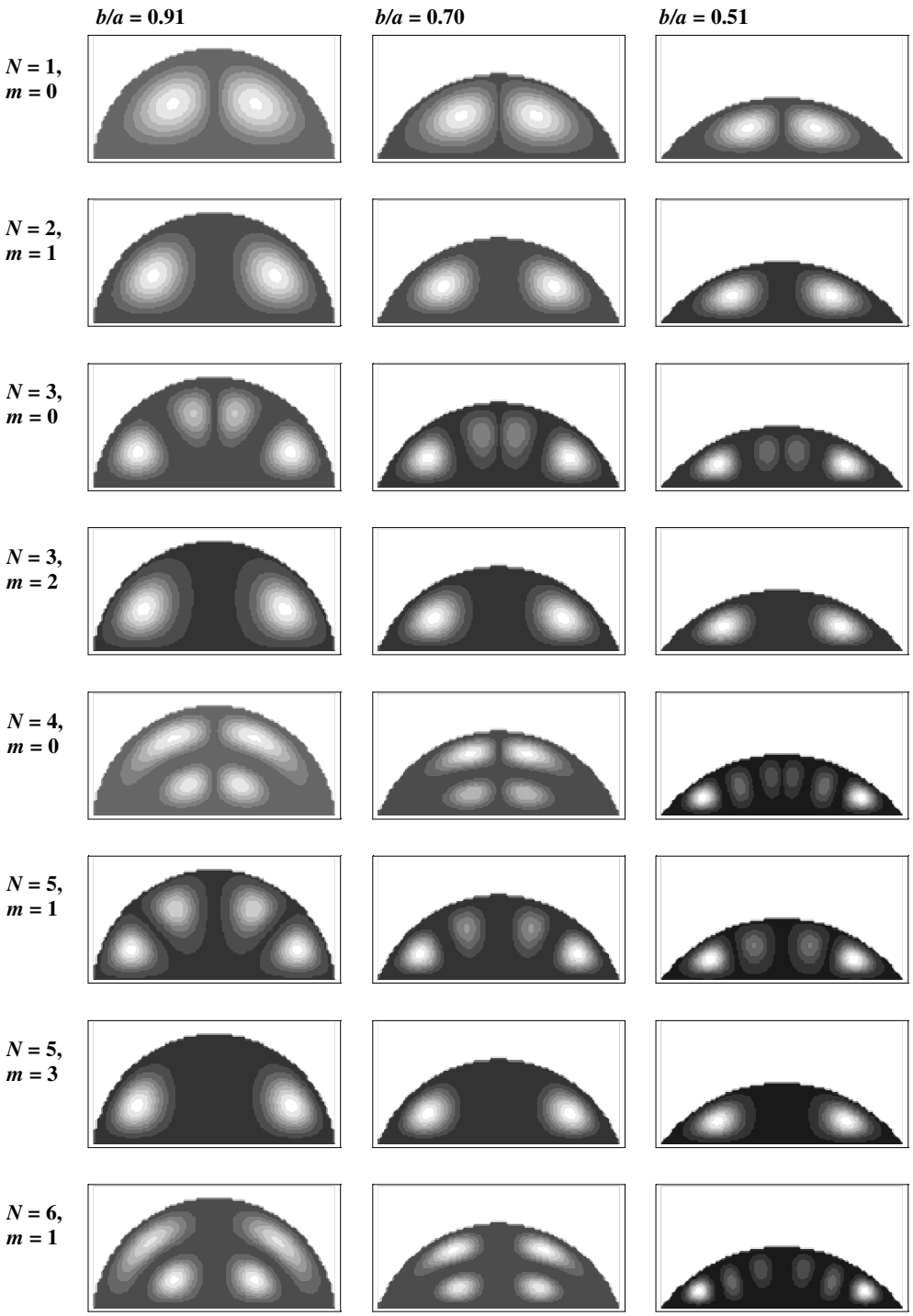

Figure 3. Contour plots for the PDF for the first eight energy levels for three different values of b/a. The white and black zones correspond to the maximum and minimum probabilities, respectively.

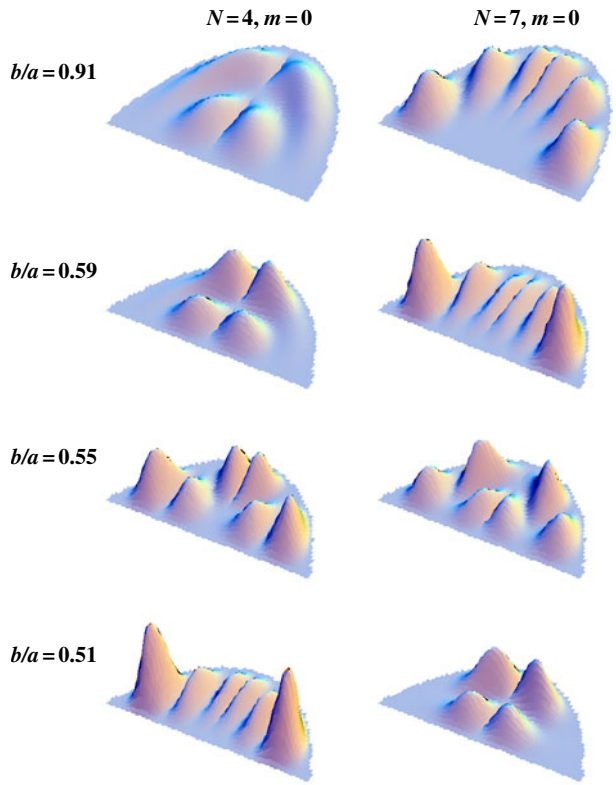

Figure 4. Three-dimensional plots for the PDF for the levels $N = 4$, $m = 0$ and $N = 7$, $m = 0$ for $b/a = 0.91, 0.59, 0.55$, and 0.51. The states represented are indicated with full dots in figure 1(a). (This figure is in colour only in the electronic version)

of all states exhibits full symmetry with a degeneracy of order l. In our case the five-fold degenerate states are $N = 7, m = 0, \pm 2$, and ± 4 ($l = 5$ at $b/a = 1$) and the other, lower in energy, is $N = 4, m = 0$ ($l = 1$ at $b/a = 1$). As b/a decreases to the value 0.91, the degenerate states split in energy but as b/a is further decreased, the two states with $m = 0$ tend to cross with each other; however, this crossing is prevented by the strong mixing of both states. This is illustrated in figure 4, where the change of the nodal distribution of the PDFs at $b/a = 0.55$ characterizes the anticrossing between these two levels. Finally, for a value of the ratio $b/a = 0.51$, beyond the anticrossing region, it is clearly seen that the functions $|f^{(\beta)}_{N,m}(\mathbf{r})|^2$ of the two even states have exchanged completely their properties.

When solving equation (7) for finding the eigenfunctions $\{C^{(\beta)}_i\}$, it is necessary to work with a matrix larger than 100×100 in order to obtain for the wavefunctions an accuracy higher than 10^{-3}. The stability problem for the eigenfunctions have a slower convergence ratio than the corresponding eigenvalue. The graphics shown in figures 3 and 4 involve an accuracy of 10^{-3}.

3. A moment quantization approach

In a previous work (see [11]), the EMM was used to generate converging lower and upper bounds, for the ground state energies, within each azimuthal quantum number symmetry class.

Excellent results were achieved, particularly for the singular thin lens regime, $b/a \to 0$. Since the EMM formulation corresponds to an affine map invariant variational procedure, there is some commonality between this method and the conformal methods previously described. It is of great interest to determine the effectiveness of the EMM procedure as applied to the excited states of the QL problem. However, the present application presents two difficulties. The first corresponds to signature issues of the wavefunction. The second concerns the adoption of the appropriate normalization prescription within EMM, as applied to excited states. For these reasons, the present formulation of EMM is a bit more complicated than that presented in [11]. The general structure of the EMM formalism is discussed in the appendix, for completeness and simplification of the relevant analysis.

In order to implement EMM, one must know the signature structure of the desired physical state. This is immediately attainable for the ground state within each azimuthal quantum number subspace. Specifically, these states can be represented in terms of nonnegative, configuration space, wavefunctions. Their moments satisfy a (moment equation (ME)) recursion relation involving the energy as an unknown parameter. The physical energy is then determined by assessing which energy values admit moment-representation solutions consistent with the well known *Moment Problem* positivity constraints [25], as incorporated within EMM. In this manner, converging lower and upper bounds to the corresponding ground state energy are obtained. As noted, this approach proved very effective [11] in analysing the thin lens limit (i.e. $b/a \to 0$). Given the affine map invariant feature of EMM, as well as its ability to generate (tight) converging bounds, such a quantization procedure defines an important computational tool for tackling singular and multiscale problems, which are usually very delicate to solve (i.e. producing varying results based on the methods used). For this reason, it is of great interest to gauge EMM's effectiveness with regards to generating the excited states of the QL problem, thereby serving to confirm the reliability of the numerical results obtained by other methods, as detailed in the previous discussion, and represented in figures 1 and 2.

3.1. Extension to excited states: the 'c'-shift EMM procedure

We refer the reader to the appendix for a comprehensive review of the essentials of the EMM formalism. Most of the following discussion makes implicit reference to the overview in the appendix. We now show how to adapt this to the present problem of solving for the excited states of the QL geometry. In the case of excited states, the wavefunctions, Φ_{exc}, (generally) have an unknown signature structure, making a straightforward implementation of EMM impossible. However, we can circumvent this difficulty and use EMM to bound the desired eigenenergies (provided certain empirical assumptions are satisfied, as will be clarified below).

We assume a lens shaped region [11] bounded by a spherical surface and an intersecting plane. The base of the lens is displaced at a distance R_1 from the origin, and the radius of curvature of the spherical surface is denoted by R_2. Note that $a^2 = R_2^2 - R_1^2$ and $b \equiv R_2 - R_1$. For reasons given in the above-referenced work, one transforms the lens region in Cartesian space into the triangular region, $\mathcal{D}$, defined by

$$\omega \equiv R_2^2 - r^2, \qquad \nu \equiv z^2 - R_1^2, \tag{9}$$

satisfying

$$0 \leqslant \omega \leqslant a^2, \qquad 0 \leqslant \nu \leqslant a^2 - \omega. \tag{10}$$

3.2. The moment equation

Within the cylindrical coordinate representation (with azimuthal angle ϕ), for simplicity, the wavefunction becomes $\Phi(r, \phi, z) \equiv e^{im\phi}\psi(r, z)$. Within the EMM approach, we work with the modified expression [11]

$$\phi(r, z) = r^m \psi(r, z), \tag{11}$$

and proceed to generate the two-dimensional ME, on the domain $\mathcal{D}$:

$$-\frac{E}{4}u(p,q) = R_2^2 p(p-1)u(p-2,q) - \left[mp + p^2 + \frac{3p}{2} + 2pq\right]u(p-1,q) \\ - 2R_1^2 pqu(p-1,q-1) + \left[q^2 + \frac{q}{2}\right]u(p,q-1) + R_1^2 q(q-1)u(p,q-2), \tag{12}$$

where $p, q \geqslant 1$, and

$$u(p,q) \equiv \int\int_{\mathcal{D}} d\omega\, d\nu\, \omega^p \nu^q \phi(\rho(\omega,\nu), z(\omega,\nu)), \tag{13}$$

with no assumed normalization prescription.

The above ME is a homogeneous, linear, recursive relation in which specification of the initialization variables, $\{u(0,0), u(0,1), \ldots, u(0,I)\} \cup \{u(1,0), u(2,0), \ldots, u(I,0)\}$, generates all the moments within the square region: $\{u(p,q)|(p,q) \in [0,I]\times[0,I]\}$. We refer to the initialization variables as *missing moments* and designate them by $\{\chi_\ell|0 \leqslant \ell \leqslant 2I\}$. The missing moment sequence ordering, $\{\ell = 0, 1, 2, \ldots, I, I+1, \ldots, 2I\}$, corresponds to the missing moment ordering $\{u(0,0), u(0,1), u(0,2), \ldots, u(0,I), u(1,0), \ldots, u(I,0)\}$, respectively. For future reference, we will also refer to the missing moment coordinate ordering as $(i_\ell, j_\ell) = (0,0), (0,1), \ldots$. In terms of the missing moments, the ME is equivalent to

$$u(p,q) = \sum_{\ell=0}^{2I} M_{p,q;\ell}(E)\chi_\ell, \tag{14}$$

where the energy dependent coefficients, $M_{p,q;\ell}(E)$, satisfy the same ME relation with respect to the p, q indices, as well as the initialization conditions

$$\text{Initialization conditions} \rightarrow \begin{cases} M_{0,n;\ell}(E) = \delta_{n,\ell}, & \text{if } 0 \leqslant n \leqslant I, \quad 0 \leqslant \ell \leqslant I, \\ M_{n,0;\ell}(E) = \delta_{n,\ell-I}, & \text{if } 1 \leqslant n \leqslant I, \quad I+1 \leqslant \ell \leqslant 2I. \end{cases} \tag{15}$$

Attention must now be given to defining an appropriate normalization condition consistent with the linear programming algorithmic structure of EMM, and its implicit preference with working with nonnegative, initialization, variables.

3.3. Developing a positive missing moment representation

For the case of nonnegative, ground state, configurations, the missing moments, restricted to the domain $\mathcal{D}$, are all positive. Thus, if one imposes the normalization $\sum_{\ell=0}^{2I} \chi_\ell = 1$, for instance, then the (unconstrained) missing moments, $\{\chi_\ell|1 \leqslant \ell \leqslant 2I\}$, must lie within the unit hypercube. This is the normalization usually adopted within the EMM approach (see appendix equations (A.8), (B.1), and (B.2)). In the case of excited states, since the missing moments are not necessarily positive, such a normalization condition does not localize the possible range of values for the missing moments. We prefer to first transform the previous formalism into an alternate moment representation, involving positive moments, and on which

a suitable normalization condition will be imposed. In order to achieve this, we must consider the following, circuitous, analysis. Let us implicitly assume that the ϕ configuration, in equation (11), is normalized according to any prescription. Let us represent the normalized configuration by the notation $\hat{\phi}$. Although the excited state configurations, $\hat{\phi}$, are real, they alternate in signature. Thus, we cannot impose the Moment Problem positivity constraints, arising within the EMM algorithm. However, one can bypass this difficulty if the quantity

$$\hat{c}_{\min} \equiv -\min\{\hat{\phi}_{\text{exc}}(\omega, \nu) | (\omega, \nu) \in \mathcal{D}\} > 0 \tag{16}$$

is known. One can then apply the EMM formalism to the nonnegative configuration, $\hat{\phi}(\omega, \nu)+\hat{c}$, for $\hat{c} \geqslant \hat{c}_{\min}$. In practice, we do not know $\hat{c}_{\min}$ for each excited state. The best we can do is empirically determine an appropriate $\hat{c}$ value, as confirmed by implementing the EMM procedure and showing that it yields a decreasing sequence of nested feasible energy intervals (manifesting convergence to a single point, the physical energy). This approach becomes an estimation method; although, in principle, if an appropriate $\hat{c}$ value has been chosen, the endpoints of the nested sequence of intervals define converging lower and upper bounds to the corresponding excited state energy. This is made possible by EMM's theoretical structure which guarantees that, if $\hat{c} < \hat{c}_{\min}$, then at some sufficiently high expansion order, I, no feasible energy interval exists.

Given the nonnegative configuration, $\hat{\phi} + \hat{c}$, for $\hat{c} \geqslant \hat{c}_{\min}$, we are free to impose any other normalization on it by multiplying by the factor $\mathcal{N}$. Thus, we can take $\phi_{\mathcal{N};\hat{c}} = \mathcal{N}(\hat{\phi} + \hat{c})$. We now define the corresponding power moments:

$$u_{\mathcal{N};\hat{c}}(p, q) = u(p, q) + \hat{c}\mathcal{N}v(p, q), \tag{17}$$

where $u_{\mathcal{N};\hat{c}}(p, q) = \int\int_{\mathcal{D}} \mathrm{d}\omega\, \mathrm{d}\nu\, \omega^p \nu^q \phi_{\mathcal{N};\hat{c}}(\omega, \nu)$, $u(p, q) = \int\int_{\mathcal{D}} \mathrm{d}\omega\, \mathrm{d}\nu\, \omega^p \nu^q \mathcal{N}\hat{\phi}(\omega, \nu)$, and

$$v(p, q) = \int\int_{\mathcal{D}} \mathrm{d}\omega\, \mathrm{d}\nu\, \omega^p \nu^q = \frac{1}{(q+1)} a^{2(p+q+2)} \int_0^1 \mathrm{d}w\, w^p (1-w)^{q+1}. \tag{18}$$

We can evaluate the last integral by simply integrating over the term ensuing from the binomial expansion of $(1-w)^{q+1}$. For notational simplicity, we define $\tilde{u}(p, q) \equiv u_{\mathcal{N};\hat{c}}(p, q)$, and $c \equiv \mathcal{N}\hat{c}$. It is the '$c$' parameter that we explicitly use in the final set of ME relations given below. Let us now substitute for $u(p, q)$ in the previous ME. We obtain

$$\begin{aligned} -\frac{E}{4}\tilde{u}(p, q) = {} & R_2^2 p(p-1)\tilde{u}(p-2, q) - \left[mp + p^2 + \frac{3p}{2} + 2pq\right]\tilde{u}(p-1, q) \\ & - 2R_1^2 pq\tilde{u}(p-1, q-1) + \left[q^2 + \frac{q}{2}\right]\tilde{u}(p, q-1) \\ & + R_1^2 q(q-1)\tilde{u}(p, q-2) + cT(p, q), \end{aligned} \tag{19}$$

for $p, q \geqslant 1$, where

$$\begin{aligned} T(p, q) = {} & -\frac{E}{4}v(p, q) - R_2^2 p(p-1)v(p-2, q) + \left[mp + p^2 + \frac{3p}{2} + 2pq\right]v(p-1, q) \\ & + 2R_1^2 pqv(p-1, q-1) + \left[q^2 + \frac{q}{2}\right]v(p, q-1) - R_1^2 q(q-1)v(p, q-2). \end{aligned} \tag{20}$$

The $\tilde{u}$-moment equation is an inhomogeneous relation, involving positive moments. If one expands the above, the $\tilde{u}$ moments will be seen to have linear contributions from the corresponding missing moments $\tilde{\chi}$, as well as additional inhomogeneous contributions linearly proportional to c. This can be rewritten as

$$\tilde{u}(p, q) = \sum_{\ell=0}^{2I} \tilde{M}_{p,q;\ell}(E)\tilde{\chi}_\ell + c\mathcal{I}_{p,q}(E), \tag{21}$$

where the $\tilde{M}$ coefficients satisfy the above ME (without the c term), and the initialization conditions are as specified before. The inhomogeneous term, $\mathcal{I}_{p,q}(E)$, will satisfy the ME, with the T terms kept, as well as the initialization conditions (i.e. as required by self consistency for the missing moments)

$$\begin{aligned} &\mathcal{I}_{0,n} = 0, \qquad \text{if } 0 \leqslant n \leqslant I, \\ &\mathcal{I}_{n,0} = 0, \qquad \text{if } 1 \leqslant n \leqslant I. \end{aligned} \tag{22}$$

Alternatively, since $\chi_\ell = \tilde{\chi}_\ell - cv(i_\ell, j_\ell)$, we have

$$\tilde{u}(p,q) - cv(p,q) = \sum_{\ell=0}^{2I} M_{p,q;\ell}(E)(\tilde{\chi}_\ell - cv(i_\ell, j_\ell)), \tag{23}$$

which becomes

$$\tilde{u}(p,q) = \sum_{\ell=0}^{2I} M_{p,q;\ell}(E)\tilde{\chi}_\ell + c\left(v(p,q) - \sum_{\ell=0}^{2I} M_{p,q;\ell}(E)v(i_\ell, j_\ell)\right). \tag{24}$$

Thus, we see that $\tilde{M}_{p,q;\ell}(E) = M_{p,q;\ell}(E)$, and $\mathcal{I}_{p,q} = v(p,q) - \sum_{\ell=0}^{2I} M_{p,q;\ell}(E)v(i_\ell, j_\ell)$.

3.4. Defining a (missing moment)-independent normalization prescription

We must still impose a normalization on the $\tilde{u}(p,q)$ (i.e. define $\mathcal{N}$). Usually, one would consider constraining the new missing moments to $\sum_{\ell=0}^{2I} \tilde{\chi}_\ell = \mathcal{A} = 1$, where the $\mathcal{A}$ parameter is explicitly introduced to suggest the general nature of such normalizations. Such a normalization procedure is implicitly different for each missing moment subspace considered. In the case of nonnegative ground states, where '$c = 0$', this is no problem. However, for multidimensional, excited state problems, in which the number of missing moments changes with the order of the calculation, the above normalization is not the preferred choice, since it would lead to an order dependent, normalization prescription, complicating the interpretation of the 'c'-shift parameter, within each missing moment subspace. That is, we prefer to work with an EMM/C-shift formalism in which (implicitly) $\hat{c}$ and $\mathcal{N}$ (and thereby 'c') are independent of the dimensionality of the missing moment subspace being used. This makes the empirical determination/assessment of 'c', as previously described, much easier. Fortunately, in the present case, where the multidimensional domain is compact, a convenient normalization prescription is possible allowing for an I-independent determination of 'c'. For compact domains, $\mathcal{D}$, it is sufficient to impose the normalization

$$\tilde{u}(0,0) = \mathcal{A} = 1. \tag{25}$$

One can normalize the desired solution this way since, assuming that $\hat{c} > \hat{c}_{\min}$, there then exists a positive normalization factor, $\mathcal{N} > 0$, which can satisfy equation (25). That is

$$\mathcal{N} \int\int_{\mathcal{D}} \mathrm{d}\omega \, \mathrm{d}\nu \, (\hat{\phi} + \hat{c}) = \mathcal{A}, \tag{26}$$

or (recalling, $c \equiv \hat{c}\mathcal{N}$)

$$c = \frac{\mathcal{A}}{(M/\hat{c}) + v(0,0)}, \tag{27}$$

where $M = \int\int_{\mathcal{D}} \mathrm{d}\omega \, \mathrm{d}\nu \, \hat{\phi}(\omega, \nu)$, $\hat{c}_{\min} < \hat{c} < \infty$, and $v(0,0) = a^4/2$. Depending on the signature of M, there are two possibilities (in units of a):

$$\frac{\mathcal{A}}{(M/c_{\min}) + (1/2)} < c < 2\mathcal{A}, \qquad \text{if } M > 0; \tag{28}$$

$$2\mathcal{A} < c < \frac{\mathcal{A}}{(M/c_{\min}) + (1/2)}, \qquad \text{if } M < 0. \tag{29}$$

Since $\mathcal{D} \subset [0, a^2] \times [0, a^2]$, and $\frac{\omega^p \nu^q}{a^{2(p+q)}} \leqslant 1$, for $(\omega, \nu) \in \mathcal{D}$, then

$$\frac{\tilde{u}(p,q)}{a^{2(p+q)}} \leqslant \tilde{u}(0,0) = \mathcal{A} = 1, \tag{30}$$

for all (p, q). Then

$$\text{New normalization} \rightarrow \begin{cases} \tilde{\chi}_\ell < 1, & \text{if } \ell \neq 0, \\ \tilde{\chi}_0 = 1. \end{cases} \tag{31}$$

The final requirement is to incorporate this normalization into the ME relation. For the above case, we have

$$\tilde{u}(p,q) = M_{p,q;0}(E) + \sum_{\ell=1}^{2I} M_{p,q;\ell}(E)\tilde{\chi}_\ell + c\mathcal{I}_{p,q}(E). \tag{32}$$

The linear programming analysis implemented in [11] can proceed unchanged, except for, effectively, incorporating the $c\mathcal{I}_{p,q}(E)$ matrix into the $M_{p,q;0}(E)$ expression. The numerical implementation of the above simply requires that, for $\mathcal{A} = 1$, we (empirically) fix c to be $c = f/v(0,0)$, and $f \approx 1$, but not equal to unity (i.e. $f \neq 1$), since then $\tilde{c} \rightarrow \infty$, and $\mathcal{N} = 0$.

3.5. Numerical results

In table 1, we give the energy estimates for $b/a = 0.6$ and $m = 0, 1, 2, 3, 4$. These estimates compare well with the plots in figure 1. Our code is not sufficiently efficient to address expansion orders $I \geqslant 4$, although some limited attempts were made in this regard. It is our expectation that the estimates given in table 1 (for the empirically determined 'c'-shift value) will hold at higher orders, thereby affirming that the feasible energy values quoted do correspond to converging bounds.

In table 2, we do the same but for $b/a = 0.5, 0.4, 0.3, 0.2$ and 0.1. The tightness of the estimates deteriorates with decreasing lens thickness.

In the cited tables, we do not implement the EMM/C-shift formalism, at the higher I-order, for the ground state, since these are already determined in [11]. The results presented in the tables demonstrate the viability of the EMM/C-shift formalism, although greater computational power (i.e. precision) is required to achieve more accurate results. Nevertheless, the numbers given confirm the accuracy of the numerical methods employed in generating figures 1 and 2. In addition, tables 1 and 2, show that the present method can be used to generate reliable results for the thin lens limit. In figure 5 we compare the EMM results with that generated through the Hill determinant approach. Although both results are very consistent and support the validity of the EMM formulation presented, we have found a small discrepancy for the $E_{4,0}$ at $b/a = 0.4$ (i.e. the result does not lie within the EMM 'bounds'). This level was calculated using a 150×150 matrix to obtain a higher precision in the CMM calculation following equation (7). A difference between both methods less than 1.5% at $b/a = 0.4$ was obtained.

We believe that this discrepancy can be attributed to a slightly poor, empirical, estimation of the corresponding 'c'-shift value used, in the pertinent EMM analysis. We remind the reader that the EMM 'c'-shift approach depends upon a good estimate of the absolute maximum of the wavefunction, $\mathcal{M}$. If $c \gg \mathcal{M}$, then the generated bounds will converge slowly. If $c < \mathcal{M}$, then at some moment expansion order, the EMM bounds disappear. The preferred case is that c be close to, but larger than, $\mathcal{M}$. Then the bounds will exhibit the fastest convergence to the physical energy. The only way to confirm, empirically, that $c > \mathcal{M}$, is to determine the existence of a nested sequence of feasible energy intervals, for arbitrarily large moment

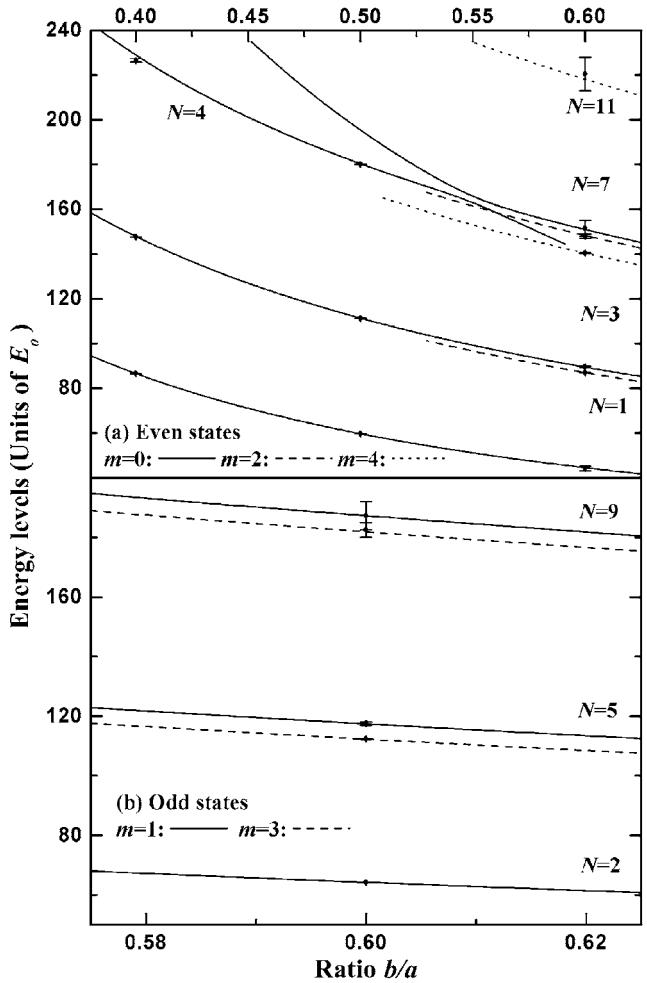

Figure 5. A comparison between the first energy levels calculated using the EMM (with empirically estimated *c-shift* parameter) and CMM approach. (a) Even states with $m = 0$, $N = 1, 3, 4, 7$ (solid lines), $m = 2$, $N = 3, 7$ (dashed lines), and $m = 4$, $N = 7, 11$ (doted lines). (b) Odd states for $m = 1$, $N = 2, 5, 9$ (solid lines) and $m = 3$, $N = 5, 9$ (dashed lines). The bounds, given in table 1, are denoted by error bars.

expansions. Clearly, this is impossible in practice. Thus, if the bounds disappear, as they might for the above $b/a = 0.4$ case (when evaluated at a higher EMM moment order, which we cannot implement within our present computational capabilities), it would confirm the inadequacy of our empirical estimate for 'c'.

Nevertheless, this one exception reveals the numerical stability of the EMM-c-shift approach. Slight deviations from the true physical values do not significantly alter the derived energy estimates.

4. Conclusions

We have shown that CMM provides formally analytical solutions for the excited states for the Helmoholtz's equation with Dirichelt boundary condition in a lens-cap region. The eigenstates

Table 1. EMM/C-shift energy estimates (bounds in units of E_0).

$\frac{b}{a}$	$f\left(c=\frac{f}{v(0,0)}\right)$	m	I	$E_{\text{Lower}} < E_{N,m} < E_{\text{Upper}}$
0.6	0.9	0	5	$43 < E_{1,0} < 46,\ 86 < E_{3,0} < \infty$
			7	$43 < E_{1,0} < 45,\ 89.1 < E_{3,0} < 89.7,\ 148 < E_{7,0} < 155$
0.6	0.8	1	5	$63 < E_{2,1} < 66,\ 110 < E_{5,1} < \infty$
			7	$64.19 < E_{2,1} < 64.27,\ 117 < E_{5,1} < 118,\ 182.5 < E_{9,1} < 192$
0.6	0.8	2	5	$84 < E_{3,2} < 89,\ 130 < E_{7,2} < \infty$
			7	$86.86 < E_{3,2} < 86.98,\ 147 < E_{7,2} < 149,\ 214 < E_{8,2} < \infty$
0.6	0.8	3	5	$109 < E_{5,3} < 117,\ 147 < E_{9,3} < \infty$
			7	$112.2 < E_{5,3} < 112.4,\ 180 < E_{9,3} < 185$
0.6	0.8	4	5	$133.4 < E_{7,4} < \infty$
			7	$140.2 < E_{7,4} < 140.5,\ 213 < E_{11,4} < 228$

Table 2. EMM/C-shift energy estimates (bounds in units of E_0).

$\frac{b}{a}$	$f\left(c=\frac{f}{v(0,0)}\right)$	m	I	$E_{\text{Lower}} < E_{N,m} < E_{\text{Upper}}$
0.5	0.8	0	5	$59.2 < E_{1,0} < 59.8,\ 108 < E_{3,0} < 129,\ 144 < E_{4,0} < \infty$
0.5	0.8	0	7	$59.54 < E_{1,0} < 59.57$, no other feasible energies
0.5	0.9	0	5	$58.9 < E_{1,0} < 60.1,\ 102 < E_{3,0} < \infty$
0.5	0.9	0	7	$59.53 < E_{1,0} < 59.58,\ 111 < E_{3,0} < 111.7,\ 173 < E_{4,0} < 191$
0.5	0.9	0	9	$111.2150 < E_{3,0} < 111.2575,\ 179.85 < E_{4,0} < 180.25$
0.4	0.9	0	5	$83 < E_{1,0} < 89,\ 130 < E_{3,0} < \infty$
		0	7	$86.36 < E_{1,0} < 86.39,\ 147 < E_{3,0} < 149,\ 211 < E_{4,0} < \infty$
		0	9	$147.54 < E_{3,0} < 147.56,\ 225.70 < E_{4,0} < 227.34$
0.3	0.9	0	5	$134 < E_{1,0} < \infty$
			7	$141.6 < E_{1,0} < 142.2,\ 213 < E_{3,0} < 233,\ 267 < E_{4,0} < \infty$
0.2	0.9	0	5	$263 < E_{1,0} < \infty$
			7	$289 < E_{1,0} < 301,\ 370 < E_{3,0} < \infty$
0.1	0.9	0	5	$920 < E_{1,0} < \infty$
			7	$995 < E_{3,0} < \infty$

and eigenvalues are given in terms of the deformation b/a with respect to the semi-spherical case. A complete set of orthogonal functions for the Dirichlet problem within the lens boundary are explicitly reported according to their symmetry properties where the space of solutions is divided into two Hilbert subspaces with well defined azimuthal angular momentum. We found that the second-order perturbation of a modified Rayleigh–Schrödinger perturbation method [17] is no longer valid for values of $b/a < 0.8$ in the case of the ground state. These values of b/a are drastically reduced when the problem of the exited states are considered, showing that perturbation methods break down even for small lens deformation. Due to the breaking of circular symmetry by the lens geometry, the eigenenergies for the same azimuthal angular momentum quantum number m correspond to anticrossings. Hence, the PDF tends to be localized to the plane $\theta = \pm\pi/2$ and its nodal structure is strongly modified as the lens deformation increases. We have shown that the excited states show anticrossing effects and strong mixing of states occurs near anticrossing points with the same value of m.

Also, for completeness, we have presented an exhaustive analysis of the excited states for the infinite QL potential problem in terms of EMM theory, within our present

computational power. The results are consistent with the results computed through the previous methods, as shown in figure 5. To the extent that the indicated c parameter value is correctly determined, empirically, the bounds given in the tables are true bounds. The only way to assess that a particular c value is incorrect is to find a missing moment subspace (i.e. expansion 'order' I) in which no feasible energy values are generated. Within our computational power, this has not been observed, thereby supporting the empirically based expectation that the quoted results correspond to true bounds.

Appendix A. Overview of the eigenvalue moment method

We present a brief overview of the essentials of the EMM formalism for multidimensional quantum problems. We assume that the Schrödinger potential corresponds to a rational polynomial. In such cases, one can transform the Schrödinger equation into an ME representation involving the power moments of the wavefunction, $\phi(\omega, \nu)$:

$$u(p, q) = \int \int_{\mathcal{D}} \mathrm{d}\omega \, \mathrm{d}\nu \, \omega^p \nu^q \phi(\omega, \nu), \tag{A.1}$$

for $p, q \geqslant 0$. We implicitly accept the possibility that the domain of definition can be other than the full two-dimensional space, $\mathcal{D} \subset \Re^2$. The major focus of the recent work by Handy *et al* [11] was to show how an EMM analysis could be implemented on a set of MEs devoid of any boundary terms (i.e. involving the wavefunction), when the domain $\mathcal{D}$ is compact.

The ME relation corresponds to a two-dimensional, linear, finite difference equation for the $u(p, q)$. An infinite subset of the moments, $\{u(m_\ell, n_\ell) | 0 \leqslant \ell < \infty\}$, serves to generate the rest of the moments through a linear relation denoted by

$$u(p, q) = \sum_{\ell=0}^{L(p,q)} M_{p,q,\ell}(E) u(m_\ell, n_\ell). \tag{A.2}$$

The M-coefficients are energy, E, dependent, and satisfy the same ME relation, with respect to the (p, q) indices, for fixed ℓ. From this, one can readily generate the M-coefficients, provided the following initialization conditions are imposed:

$$M_{p,q,\ell} = \begin{cases} 0, & \text{if } (p, q) \neq (m_\ell, n_\ell) \\ 1, & \text{if } (p, q) = (m_\ell, n_\ell). \end{cases} \tag{A.3}$$

The $\{u(m_\ell, n_\ell)\}$ moments are referred to as the *missing moments*. As suggested by the moment/missing moment relation, any finite number of the moments are generated by a corresponding finite number of missing moments. Thus, to any order within the EMM formulation, one is working, exactly, within a finite subspace of the missing moment space.

Let us assume that the physical configuration is nonnegative, $\phi(\omega, \nu) \geqslant 0$. This is always the case for any multidimensional, bosonic, ground state configuration space wavefunction. In 1985, Handy and Bessis [26] investigated the extent to which the Hankel–Hadamard (HH) determinant, positivity theorems, from the classic mathematical *Moment Problem*, could be used to quantize the energy. This investigation proved highly successful for two reasons. First, the energy was determined through the generation of converging lower and upper bounds, thereby making this moment quantization method capable of producing high accuracy results. Second, as originally argued by Handy [27], moment quantization methods proved to be relevant in addressing singular perturbation/strong coupling problems not amenable to conventional perturbation theory methods. Both of these features were confirmed by the original formulation of Handy and Bessis. However, the HH formulation involved nonlinear moment dependent constraints which proved inefficient for problems with a large number

of missing moments. In 1988, Handy *et al* [28] linearized the formalism in a manner that exploited the use of linear programming. This allowed application to problems with a large number of missing moments. It is this formulation that is referred to as the EMM approach.

If $\phi \geqslant 0$, on $\mathcal{D}$, then the following integrals are automatically positive:

$$\int\int_{\mathcal{D}} \left(\sum_{i,j \in \mathcal{S}_d} C_{i,j} \omega^i \nu^j \right)^2 \phi(\omega, \nu) > 0, \tag{A.4}$$

where the C's are arbitrary, so long as they are not all zero. The sets $\mathcal{S}_0 \subset \mathcal{S}_1 \subset \mathcal{S}_2 \subset \cdots \subset \mathcal{S}_d \subset \cdots \subset \mathcal{S}_\infty$ represent an appropriate, nonnegative integer, coordinate pair sequence ordering. The set $\mathcal{S}_d$ represents the first '$d + 1$' elements of this sequence. An important observation is that the above integral involves integrating ϕ with respect to a positive polynomial formed by taking the square of an arbitrary polynomial, $\mathcal{P}_C(\omega, \nu)^2$. Let $\mathcal{O}$ symbolize any two-dimensional, linear transformation $\mathcal{O}(\omega, \nu) = (\omega', \nu')$. By sampling over the space of C-tuples, we automatically sample over all possible $\mathcal{O}$-copies of $\mathcal{P}_C$. More generally, the expression $(\sum_{j=1}^{J} a_j \mathcal{P}_C(\mathcal{O}_j(\omega, \nu)))^2$, for arbitrary a_j and $\mathcal{O}_j$, corresponds to a polynomial within the same space as $\mathcal{P}_C$. This is an important observation which explains why EMM is invariant under all affine map transformations. We return to this point later on. Expanding and interchanging the integration and summation operations yields the quadratic form relations

$$\sum_{(i_1,j_1) \in \mathcal{S}_d} \sum_{(i_2,j_2) \in \mathcal{S}_d} C_{i_1,j_1} u(i_1 + i_2, j_1 + j_2) C_{i_2,j_2} > 0. \tag{A.5}$$

Let us also assume that $\phi = 0$ for $(\omega, \nu) \in \mathcal{C}_\mathcal{D} \equiv \Re^2 - \mathcal{D}$, and that there exists a finite set of polynomials, $\mathcal{P}_n(\omega, \nu) \equiv \sum_{l=0}^{L_n} \Gamma_{n,l} \omega^{i_{n,l}} \nu^{j_{n,l}}$, $1 \leqslant n \leqslant I$, such that the union of all subsets where these polynomials are negative corresponds to $\mathcal{C}_\mathcal{D}$:

$$\mathcal{C}_\mathcal{D} = \bigcup_{n=1}^{I} \{(\omega, \nu) | \mathcal{P}_n(\omega, \nu) < 0\}. \tag{A.6}$$

For each of these polynomials, we also have the corresponding, positivity, integral relations

$$\int\int_{\mathcal{D}} \left(\sum_{i,j \in \mathcal{S}_d} C_{i,j} \omega^i \nu^j \right)^2 \mathcal{P}_n(\omega, \nu) \phi(\omega, \nu) > 0, \tag{A.7}$$

or

$$\sum_{(i_1,j_1) \in \mathcal{S}_d} \sum_{(i_2,j_2) \in \mathcal{S}_d} \sum_{l=0}^{L_n} C_{i_1,j_1} (\Gamma_{n,l} u(i_1 + i_2 + i_{n,l}, j_1 + j_2 + j_{n,l})) C_{i_2,j_2} > 0. \tag{A.8}$$

For simplicity of notation, we will also define $\mathcal{P}_0(\omega, \nu) \equiv 1$. The above set of constraints, for all $\mathcal{P}_n$, constitute the multidimensional *Moment Problem* constraints which must be satisfied by the physical solution(s), for all C. An important part of the EMM algorithmic implementation is determining the appropriate coordinate integer pair sequence subsets, $\mathcal{S}_d$, and the corresponding missing moments. We need to determine a coordinate pair sequence $\mathcal{S}_d \equiv \{(i_\delta, j_\delta) | 0 \leqslant \delta \leqslant d\}$, so that the set of coordinate pairs $\{(i_{\delta_1}, j_{\delta_1}) + (i_{\delta_2}, j_{\delta_2}) + (i_{n,l}, j_{n,l}) | 0 \leqslant \delta_{1,2} \leqslant d, 0 \leqslant n \leqslant I, 0 \leqslant l \leqslant L_n\}$, required in the above quadratic forms, be generated by a finite set of corresponding missing moments. Let us assume that this has been done.

Appendix B. Imposing a normalization

Before substituting the moment/missing moment relation in the above set of linear inequalities, we must specify a normalization. Since the ME relation is also homogeneous, the

moment/missing moment relation, as given, does not assume any specific normalization. In implementing the EMM linear programming formulation, at each step, we work within a finite missing moment subspace, $\mathcal{M}_\Lambda \equiv \{(u(m_\ell, n_\ell)|0 \leqslant \ell \leqslant \Lambda < \infty\}$, of dimension $\Lambda + 1$. This finite set of missing moments in turn generates a finite set of power moments on which the previous linear inequality constraints are imposed. Within the $\mathcal{M}_\Lambda$ missing moment subspace, we must impose a normalization. We can take

$$\sum_{\ell=0}^{\Lambda} u(m_\ell, n_\ell) = 1. \tag{B.1}$$

If the desired physical solution is nonnegative, then this condition also constrains all of the missing moments to lie within the unit hypercube:

$$(u(m_0, n_0), \ldots, u(m_\ell, n_\ell), \ldots, u(m_\Lambda, n_\Lambda)) \in [0, 1]^{\Lambda+1}. \tag{B.2}$$

Note that the normalization in equation (B.1) changes with the dimension of the missing moment subspace being considered. This feature is unsuitable for multidimensional application of EMM analysis to excited states, as discussed in section 3.

In any coordinate ordering scheme, the zeroth-order moment will almost always be the starting missing moment. Assuming this, we solve for $u(0, 0)$ in terms of the other, unconstrained, missing moments:

$$u(0, 0) = 1 - \sum_{\ell=1}^{\Lambda} \chi_\ell, \tag{B.3}$$

where we have defined $\chi_\ell \equiv u(m_\ell, n_\ell)$, for simplicity of notation ($\chi_0 \equiv 1$). Incorporating this within the moment/missing moment relation gives us the normalized expression

$$u(p, q) = \hat{M}_{p,q,0}(E)\chi_0 + \sum_{\ell=1}^{\Lambda} \hat{M}_{p,q,\ell}(E)\chi_\ell, \tag{B.4}$$

for all (p, q) pairs whose associated moments are generated by the first $\Lambda + 1$ sequence of missing moments. The required coefficients must satisfy

$$\hat{M}_{p,q,0}(E) = M_{p,q,0}(E) \tag{B.5}$$

and

$$\hat{M}_{p,q,\ell}(E) = M_{p,q,\ell}(E) - M_{p,q,0}(E), \tag{B.6}$$

$1 \leqslant \ell \leqslant \Lambda$. Substituting the above normalized moment/missing moment relation into the quadratic form expression gives

$$\sum_{\delta_1=0}^{d} \sum_{\delta_2=0}^{d} \sum_{l=0}^{L_n} C_{i_{\delta_1}, j_{\delta_1}} (\Gamma_{n,l} u(i_{\delta_1} + i_{\delta_2} + i_{n,l},\, j_{\delta_1} + j_{\delta_2} + j_{n,l})) C_{i_{\delta_2}, j_{\delta_2}} > 0, \tag{B.7}$$

or

$$\sum_{\ell=0}^{\Lambda} \chi_\ell \left(\sum_{\delta_1=0}^{d} \sum_{\delta_2=0}^{d} \sum_{l=0}^{L_n} C_{i_{\delta_1}, j_{\delta_1}} (\Gamma_{n,l} \hat{M}_{i_{\delta_1}+i_{\delta_2}+i_{n,l}, j_{\delta_1}+j_{\delta_2}+j_{n,l},\ell}(E)) C_{i_{\delta_2}, j_{\delta_2}} \right) > 0. \tag{B.8}$$

These then define the linear programming relations ($\chi_0 \equiv 1$)

$$\sum_{\ell=1}^{\Lambda} \mathcal{A}_{C,\ell} \chi_\ell < \mathcal{B}_C, \tag{B.9}$$

where

$$\mathcal{A}_{C,\ell} \equiv -\sum_{\delta_1=0}^{d} \sum_{\delta_2=0}^{d} \sum_{l=0}^{L_n} C_{i_{\delta_1}, j_{\delta_1}} (\Gamma_{n,l} \hat{M}_{i_{\delta_1}+i_{\delta_2}+i_{n,l}, j_{\delta_1}+j_{\delta_2}+j_{n,l},\ell}(E)) C_{i_{\delta_2}, j_{\delta_2}} \tag{B.10}$$

and

$$\mathcal{B}_C \equiv \sum_{\delta_1=0}^{d}\sum_{\delta_2=0}^{d}\sum_{l=0}^{L_n} C_{i_{\delta_1},j_{\delta_1}}(\Gamma_{n,l}\hat{M}_{i_{\delta_1}+i_{\delta_2}+i_{n,l},j_{\delta_1}+j_{\delta_2}+j_{n,l},0}(E))C_{i_{\delta_2},j_{\delta_2}}. \tag{B.11}$$

We emphasize, once more, that the linear programming variables are restricted to lie within the unit interval: $0 < \chi_\ell < 1$.

The computational objective, with respect to equation (A.7), is, in principle, to determine those E values which admit a χ solution to the above inequalities, for arbitrary C. For any E, the EMM *cutting method* determines an optimal, finite set, of C-vectors which tell us if there exists, or not, a χ solution set to the above. To order Λ (which is proportional to d), the feasible energy interval, $(E_{\min}^{(\Lambda)}, E_{\max}^{(\Lambda)})$, is determined. At the next expansion order ($\Lambda \to \Lambda + 1$), this energy interval become smaller, $(E_{\min}^{(\Lambda+1)}, E_{\max}^{(\Lambda+1)}) \subset (E_{\min}^{(\Lambda)}, E_{\max}^{(\Lambda)})$. The endpoints of these nested intervals define the converging lower and upper bounds to the physical energy:

$$\cdots < E_{\min}^{(\Lambda)} \leqslant E_{\min}^{(\Lambda+1)} < \cdots < E_{\text{ground}} < \cdots < E_{\max}^{(\Lambda+1)} \leqslant E_{\max}^{(\Lambda)} \cdots. \tag{B.12}$$

The details of the linear programming based, EMM algorithm, are left to the various cited works.

Appendix C. Affine map invariance of the EMM variational procedure

To say that a function is positive is to affirm that at every spatial point the function is positive. In this sense, positivity is a local characteristic. Clearly, to check that a function is positive, it would be very inefficient to verify this point by point, particularly for multidimensional configurations. A more efficient approach is to test for positivity by sampling first at larger (∞) scales, and then systematically at smaller scales. The theorems underlying the EMM formalism implicitly involve this type of multiscale analysis, sampling at coarse length scales and proceeding to finer scales. The exact manner that this happens is not manifest in the relations given above. We provide an intuitive analysis as to how this is achieved.

Wavelet analysis focuses on a similar procedure in order to recover the local structure of a configuration from its large scale behaviour. Thus, the scaling transform [29]

$$\underline{S\phi}(\tau_1, \tau_2, a) \equiv \frac{1}{a^2\nu(0,0)}\int\int \mathrm{d}\omega\,\mathrm{d}\nu\, S\left(\frac{\omega-\tau_1}{a}, \frac{\nu-\tau_2}{a}\right)\phi(\omega,\nu), \tag{C.1}$$

involving a bounded (positive) scaling function, $S(\omega, \nu)$, with non-zero moment, $\nu(0,0) \equiv \int\int \mathrm{d}\omega\,\mathrm{d}\nu\, S(\omega,\nu) \neq 0$, yields the wavefunction, in the zero scale limit

$$\lim_{a\to 0}\underline{S\phi}(\tau_1,\tau_2,a) = \phi(\tau_1,\tau_2). \tag{C.2}$$

If, for simplicity, we let the scaling function correspond to the Gaussian, $S(\omega,\nu) = (\exp(-\frac{(\omega^2+\nu^2)}{2}))^2$, then for most physical configurations, the corresponding scaling transform will be analytic in the inverse scale variable. Let us initiate this analysis by considering the expansion $\frac{1}{a^2\nu(0,0)}S(\frac{\omega-\tau_1}{a}, \frac{\nu-\tau_2}{a}) = \frac{1}{a^2}(\sum_{n=0}^{\infty}(\frac{1}{a^2})^n P_{n,\tau_1,\tau_2}(\omega,\nu))^2$, where P_{n,τ_1,τ_2} denotes the underlying polynomials with coefficients dependent on $\tau_{1,2}$. The truncated expansion, $\frac{1}{a^2\nu(0,0)}S(\frac{\omega-\tau_1}{a}, \frac{\nu-\tau_2}{a}) \approx \frac{1}{a^2}(\sum_{n=0}^{I}(\frac{1}{a^2})^n P_{n,\tau_1,\tau_2}(\omega,\nu))^2$, is a polynomial. For some sufficiently small scale value, and some sufficiently large I, upon multiplying this expansion by ϕ and integrating over all space, one can approximate $\phi(\tau_1,\tau_2)$. Clearly, the EMM relations include such expressions in their sample space, thereby allowing one to test, locally, for violations of positivity.

Of course, the EMM relations do much more than this. They also test for violations of positivity at larger scales. In principle, testing for positivity must be done at every location, over all scales around that location (proceeding from the coarser length scales down to

the finer scales). This is clearly a very demanding procedure. However, if one uses the space of polynomials as the sample 'test' space for positivity, the fact that such spaces are automatically invariant under all affine transforms facilitates this process. That is, under an affine transform (i.e. translations, rescalings, rotations, inversions, or any combination of these), symbolized by the notation $\mathcal{O} : (\omega, \nu) \rightarrow (\omega', \nu')$, polynomials map into polynomials ($\mathcal{P}(\mathcal{O}(\omega, \nu)) = \mathcal{P}'(\omega, \nu)$). Therefore, when we sample over all C-tuple values, as reflected in the EMM inequality constraints, we are actually including all possible affine map transforms of any given test polynomial.

The above has a real practical significance. The first multidimensional application of EMM was to the notoriously singular, quadratic Zeeman effect for hydrogenic atoms in superstrong magnetic fields. Many investigations yielded significantly varying results. In 1983, Le Guillou and Zinn-Justin developed a conformal expansion, hypervirial analysis, which attempted to generate high accuracy estimates for the ground state's binding energy [30]. The EMM bounds [28] confirmed their results. The tightness of the EMM bounds matched the estimated precision of the results by Le Guillou and Zinn-Justin. It is conjectured that the underlying reason for this is the affine map invariant structure of EMM's variational formulation. This deep relationship between EMM and conformal analysis should also be relevant to the present problem of the QL potential.

References

[1] Yoffe A D 2001 *Adv. Phys.* **50** 1
[2] Fafard S, Leon R, Leonard D, Merz J L and Petroff P M 1994 *Phys. Rev.* B **50** 8086
[3] Marzin J-Y, Gérard J-M, Izraël A, Barrier D and Bastard G 1994 *Phys. Rev. Lett.* **73** 716
[4] Grundmann M, Christen J, Ledentsov N N, Böhrer J, Bimberg D, Ruvimov S S, Werner P, Richter U, Gösele U, Heydenreich J, Ustinov V M, Egorov A Yu, Zhukov A E, Kop'ev P S and Alferov Zh I I 1995 *Phys. Rev. Lett.* **74** 4043
[5] Leon R, Petroff P M, Leonard D and Fafard S 1995 *Science* **267** 1966
[6] Leonard D, Pond K and Petroff P M 1994 *Phys. Rev.* B **50** 11687
[7] Eaglesham D J and Cerullo M 1990 *Phys. Rev. Lett.* **64** 1943
[8] Moison J M, Houzay F, Barthe F, Leprince L, Andre E and Vatel O 1996 *Appl. Phys. Lett.* **64** 195
[9] Liao X Z, Zou J, Duan X F, Cockayne D J H, Leon R and Lobo C 1998 *Phys. Rev.* B **58** R4235
[10] Zhu J H, Brunner K and Abstreiter G 1998 *Appl. Phys. Lett.* **72** 424
[11] Handy C R, Trallero-Giner C and Rodríguez A H 2001 *J. Phys. A: Math. Gen.* **34** 10991
[12] Drexler H, Leonard D, Hansen W, Kotthaus J P and Petroff P M 1994 *Phys. Rev. Lett.* **73** 2252
[13] Miller B T, Hansen W, Manus S, Luyhen R J, Lorke A and Kotthaus J P 1997 *Phys. Rev.* B **56** 6764
[14] Medeiros-Ribeiro G, Pikus F G, Petroff P M and Efros A L 1997 *Phys. Rev.* B **55** 1568
[15] Lee S, Kim J C, Rho H, Kim C S, Smith L M, Jackson H E, Furdina J K and Dobrowolka M 2000 *Phys. Rev.* B **61** 2405
[16] Cingolani R and Rinaldi R 1993 *Riv. Nuovo Cimento* **16** 1
[17] Rodríguez A H, Trallero-Giner C, Ulloa S E and Mar ín-Antuña J 2001 *Phys. Rev.* B **63** 125319
[18] Berry M V 1986 *J. Phys. A: Math. Gen.* **19** 2281
[19] Berry M V and Robnik M 1986 *J. Phys. A: Math. Gen.* **19** 1365
[20] Berry M V and Robnik M 1986 *J. Phys. A: Math. Gen.* **19** 649
[21] Itzykson C, Moussa P and Luck J M 1986 *J. Phys. A: Math. Gen.* **19** L111
[22] Robnik M 1984 *J. Phys. A: Math. Gen.* **17** 1049
[23] Bender C M and Orszag S A 1978 *Advanced Mathematical Methods for Scientists and Engineers* (New York: McGraw-Hill)
[24] Trallero-Herrero C A, Trallero-Giner C, Ulloa S E and Perez-Alvarez R 2001 *Phys. Rev.* E **64** 056237
[25] Shohat J A and Tamarkin J D 1963 *The Problem of Moments* (Providence, RI: American Mathematical Society)
[26] Handy C R and Bessis D 1985 *Phys. Rev. Lett.* **55** 931
[27] Handy C R 1981 *Phys. Rev.* D **24** 378
[28] Handy C R, Bessis D, Sigismondi G and Morley T D 1988 *Phys. Rev. Lett.* **60** 253
[29] Handy C R and Murenzi R 1999 *J. Phys. A: Math. Gen.* **32** 8111
[30] Le Guillou J C and Zinn-Justin J 1983 *Ann. Phys.* **147** 57